A&A 602, L13 (2017)
DOI: 10.1051/0004-6361/201731060

Astronomy & Astrophysics

Letter to the Editor

The intricate Galaxy disk: velocity asymmetries in *Gaia*-TGAS

T. Antoja[1], J. de Bruijne[2], F. Figueras[1], R. Mor[1], T. Prusti[2], and S. Roca-Fàbrega[3]

[1] Dept. FQA, Institut de Ciencies del Cosmos (ICCUB), Universitat de Barcelona (IEEC-UB), Marti Franques 1, 08028 Barcelona, Spain
e-mail: tantoja@fqa.ub.edu
[2] Directorate of Science, European Space Agency (ESA-ESTEC), PO Box 299, 2200 AG Noordwijk, The Netherlands
[3] Racah Institute of Physics, The Hebrew University of Jerusalem, Edmond J. Safra Campus, Givat Ram, Kaplun building, office 110, 91904 Jerusalem, Israel

Received 28 April 2017 / Accepted 1 June 2017

ABSTRACT

We use *Gaia*-TGAS data to compare the transverse velocities in Galactic longitude (coming from proper motions and parallaxes) in the Milky Way disk for negative and positive longitudes as a function of distance. The transverse velocities are strongly asymmetric and deviate significantly from the expectations for an axisymmetric galaxy. The value and sign of the asymmetry changes at spatial scales of several tens of degrees in Galactic longitude and about 0.5 kpc in distance. The asymmetry is statistically significant at 95% confidence level for 57% of the region probed, which extends up to ∼1.2 kpc. A percentage of 24% of the region shows absolute differences at this confidence level larger than 5 km s^{-1} and 7% larger than 10 km s^{-1}. The asymmetry pattern shows mild variations in the vertical direction and with stellar type. A first qualitative comparison with spiral arm models indicates that the arms are probably not the main source of the asymmetry. We briefly discuss alternative origins. This is the first time that global all-sky asymmetries are detected in the Milky Way kinematics beyond the local neighbourhood and with a purely astrometric sample.

Key words. Galaxy: disk – Galaxy: evolution – Galaxy: kinematics and dynamics – Galaxy: structure

1. Introduction

The scientific community studying the Galaxy welcomed with high expectations the publication of the first *Gaia* data (Gaia Collaboration 2016a,b) in September of 2016. Even with the limitations of the first release, the *Gaia* data possess exciting possibilities for new discoveries on the formation, evolution, and current structure of the Milky Way. The *Tycho-Gaia* astrometric solution (TGAS, Michalik et al. 2015) is the largest astrometric sample to date and comprises proper motions and parallaxes of unprecedented accuracy for two million stars.

Following the approach proposed in Antoja et al. (2016; hereafter A16), here we compare the transverse velocities in Galactic longitude (i.e. coming from proper motions and parallaxes) for negative and positive Galactic longitudes as a function of distance with the *Gaia*-TGAS data. When the solar motion is subtracted, the data reveal clear large-scale velocity asymmetries that are signatures of the non-axisymmetry in the Galaxy.

This discovery adds to recent findings of the intricacy of the Galactic disk. For instance, there is multiple evidence of radial and vertical velocity gradients and wave-like motion in the disk (e.g. Siebert et al. 2011; Widrow et al. 2012). Carlin et al. (2013) also found asymmetric vertical and radial velocities for different azimuths in the direction of the anti-centre. Recently, Bovy (2017) found evidence of non-zero values of the local divergence and radial shear while measuring the Oort constants with TGAS, but restricted to a local sample (∼200 pc). So far, these detections have been either very local, limited to the directions probed with the particular ground-based survey, or detected primarily in radial velocity data. Thanks to *Gaia*, this is the first time that we detect global all-sky velocity asymmetries beyond the local neighbourhood and with a purely astrometric sample.

We describe the data in Sect. 2 and the method in Sect. 3. We show our results on the velocity asymmetry in Sect. 4. We perform tests to asses the limitations and robustness of our results in Sect. 5. In Sect. 6 we conclude and comment on the possible origin of the detected asymmetry.

2. Data

We used proper motions from *Gaia*-TGAS (Gaia Collaboration 2016a; Lindegren et al. 2016) and the distance estimations from Astraatmadja & Bailer-Jones (2016). These were obtained in a Bayesian way from the TGAS parallaxes using different priors: i) an isotropic prior with an exponentially decreasing space density with increasing distance with a short scale length (hereafter dist1); ii) with a longer scale length (dist2); and iii) an anisotropic prior derived from the observability of stars in a Milky Way model (dist3). We also compare the results with the inverse of the parallax as a distance estimator.

We selected different layers in Z. We assumed a solar height above the plane of $Z_\odot = 0.027$ kpc (Chen et al. 2001). Our primary sample is a disk layer with $|Z| < 0.1$ kpc, and it has 936861 stars. We furthermore divided our primary sample into groups of different spectral types and luminosity classes obtained from the catalogue of Pickles & Depagne (2010), which we cross-matched with TGAS using the *Tycho*2 ID. We studied young main-sequence stars (OBAV, 66446 stars), main-sequence stars (FGKMV, 509874 stars), and giant stars (KMIII, 126988 stars).

For these samples we computed the observed transverse velocity in the longitude direction (hereafter transverse velocity) $V_\ell^{\rm obs} \equiv \kappa d \mu_{\ell *}$, where d is the distance, $\kappa = 4.74047$ is the constant for the change of kpc mas yr^{-1} to km s^{-1}, and

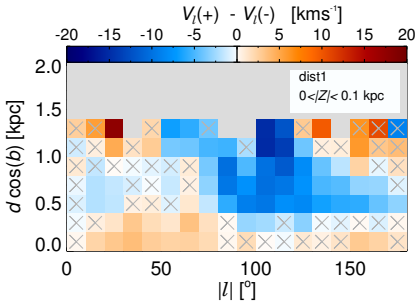

Fig. 1. Difference between the median transverse velocity in Galactic longitude as a function of longitude and distance for symmetric Galactic longitudes $\ell > 0$ and $\ell < 0$. We use bins of $\Delta d\cos(b) = 0.2$ kpc and $\Delta\ell = 10°$. We plot a grey cross in bins where $V_\ell(+) - V_\ell(-)$ is statistically consistent with 0 with a 95% confidence, i.e. where the observations are compatible with an axisymmetric galaxy. The grey region shows bins with insufficient data (we require at least five stars in each $\ell > 0$ and $\ell < 0$ bin). We have fixed the colour scale to 20 km s^{-1}.

$\mu_{\ell*} \equiv \mu_\ell \cos(b)$ is the proper motion in Galactic longitude. The median error in $V_\ell^{\rm obs}$ for the primary sample is 6 km s^{-1}, and 75% of the stars have errors smaller than 10 km s^{-1}. This velocity can be corrected for the solar motion with

$$V_\ell = V_\ell^{\rm obs} - U_\odot \sin\ell + V_\odot \cos\ell. \quad (1)$$

3. Method

Our procedure consists of comparing the median velocity of symmetric Galactic longitudes, that is, ℓ and $-\ell$, in bins of longitude and distance on the Galactic plane (ℓ, $d\cos(b)$). That is

$$V_\ell(+) - V_\ell(-) \equiv \widetilde{\kappa d\mu_{\ell*}}\,(\ell > 0) - \widetilde{\kappa d\mu_{\ell*}}\,(\ell < 0) - 2U_\odot \sin|\ell|, \quad (2)$$

where the $V_\odot \cos\ell$ term from Eq. (1) cancels out. In an axisymmetric galaxy, V_ℓ is symmetric in ℓ, and we therefore expect that $V_\ell(+) - V_\ell(-) = 0$. Non-null values of $V_\ell(+) - V_\ell(-)$ show the contribution of the non-axisymmetries. We note that asymmetries in the Galactic radial and azimuthal velocities may both contribute. This method has the advantage of being model-independent. Only an assumption on $U_\odot$ is required. We assumed $U_\odot = 9$ km s^{-1} (similar to determinations of Coşkunoğlu et al. 2011; Pasetto et al. 2012, but see discussion in Sect. 5). Asymmetries in $V_{\rm b}^{\rm obs} \equiv \kappa d\mu_{\rm b}$ are postponed to a forthcoming paper.

We estimated the 95% confidence band of $V_\ell(+) - V_\ell(-)$ with bootstrapping. We only considered bins with at least five stars (thus ten stars in the pair $\ell > 0$ and $\ell < 0$). The typical dispersion of the bootstrapped median $\widetilde{\kappa d\mu_{\ell*}}$ (indicative of the precision of the median) is 0.3 and 0.9 km s^{-1} at a distance of 0.5 and 1 kpc, respectively. This is much smaller than the individual stellar errors (Sect. 2) because of the large number of stars in each bin.

4. Tangential velocity asymmetry

In Fig. 1 we plot[1] $V_\ell(+) - V_\ell(-)$ as a function of longitude and distance on the plane for the primary sample using dist1 (see Sect. 5 for consistency with other distance estimates). Bins marked with crosses have values compatible with 0 given their 95% confidence band. For an axisymmetric galaxy, one would expect values compatible with 0 everywhere in this plot, but we see that 57% of the bins probed present an unbalanced tangential motion that is statistically significant at 95% level, that is, positive or negative $V_\ell(+) - V_\ell(-)$. If the distribution of errors in $V_\ell(+) - V_\ell(-)$ were Gaussian and the Galaxy were axisymmetric, only 5% of bins would deviate from 0 at this level of confidence, which is far lower than the measured fraction.

An alternative test to the hypothesis of axisymmetry is to assume that the distribution of $V_\ell(+) - V_\ell(-)$ for an axisymmetric galaxy is a Gaussian centred at 0 with a sigma derived from the actual data. We made 500 bootstraps of the median V_ℓ at each bin, obtaining effectively 124750 bootstrapped $V_\ell(+) - V_\ell(-)$ (combinations without repetition) for each pair of bins, from which we computed σ. Given the measured $V_\ell(+) - V_\ell(-)$ and the assumed distribution under the null hypothesis, we find that 71% of bins deviate from axisymmetry at the 95% level ($p < 0.05$). By combining all the individual p values with the Fisher's method, we infer that the hypothesis of axisymmetry can be rejected with a p value <0.001.

The asymmetry is such that the median velocity difference oscillates between –15 and 18 km s^{-1}, has a median (of absolute values) of 2.6 km s^{-1} , and a median absolute deviation (MAD) of 2.7 km s^{-1} (considering all bins). The median asymmetry is lowest (1.4 km s^{-1}) for the distance between 0.2 and 0.4 kpc, and highest (8.8 km s^{-1}) at a distance between 1.2 and 1.4 kpc. It is lowest (1.2 km s^{-1}) at longitudes of ±5° and highest (15 km s^{-1}) at longitudes of ±105°. A percentage of 47% of all bins show absolute differences larger than 2 km s^{-1} that are statistically significant at the 95% level, 24% larger than 5 km s^{-1}, and 7% larger than 10 km s^{-1}. All these numbers indicate that the kinematics of a great fraction of the solar peripheral region shows signs of non-axisymmetry.

The differences in transverse velocity of Fig. 1 show a pattern of a scale of several tens of degrees and about 0.5 kpc in distance. We observe a large region of negative differences (plotted in blue) in the range $|\ell| \sim [70, 180]°$. The positive differences (plotted in red) are mostly located at close distances, and in the inner and outer disk directions at the farthest distances probed.

Figure 2 shows the velocity asymmetries for different layers in Z as indicated in the legends. The asymmetry extends at least up and down in the plane to $|Z| = 300$ pc. Beyond this height, it looses significance because of the lack of data. We find a mild dependence on Z. The region with negative asymmetry for $|\ell| \gtrsim 70°$ is present at all Z, but there is a large region with positive asymmetry at $|\ell| \lesssim 70°$ that is only present at the higher Z probed. Beyond $|Z| > 100$ pc, the asymmetry seems to be dominated by a duality of positive and negative asymmetry, while most of the small-scale pattern is significant only at low Z. We do not find differences with small changes in the $Z_\odot$ assumed.

Figure 3 shows the velocity asymmetries for the different stellar groups described in Sect. 2 (except for the FGKV since it looks essentially as Fig. 1.). Interestingly, the large blue region of negative differences appears for all sub-samples, but the asymmetry differs substantially in the inner parts of the Galaxy ($\ell \lesssim 70$): it is negative for the OBAV group, it is both positive and negative for the FGKMV group, and it is mostly positive for the KMIII group at the farthest distances (there is not enough statistics at closer distances for this group). The median velocity asymmetry (for statistically significant bins) is largest for the KMIII group (8 km s^{-1}), followed by the OBAV (7 km s^{-1}) and the FGKMV (5 km s^{-1}).

[1] We note that this is the same quantity as plotted in Fig. 6 of A16, which was called $\Delta - \Delta_{\rm exp}$ there. We also note that in A16 we used larger bins in distance and a different vertical range in the plots.

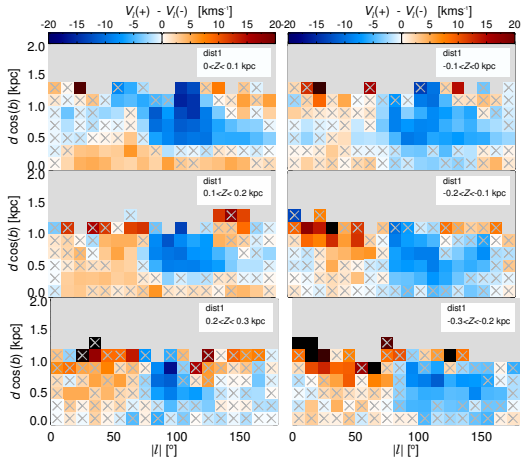

Fig. 2. Same as Fig. 1, but for different layers in Z.

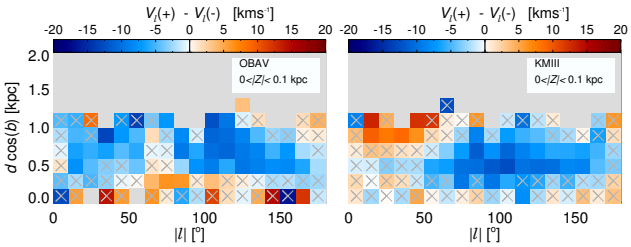

Fig. 3. Same as Fig. 1, but for different stellar types. The plot for FGKV is omitted since it looks essentially the same as Fig. 1.

5. Robustness tests

Here we perform tests to show the robustness of our results and check that the limitations of the TGAS data and of our method do not contribute to induce or increase the observed velocity asymmetry between $\ell > 0$ and $\ell < 0$.

General astrometric quality. When we select stars in the first quartile with better astrometric quality (*astrometric_excess_noise* < 0.37), we observe no significant differences with Fig. 1. The values of $V_\ell(+) - V_\ell(-)$ differ in median only by 1.4 km s^{-1}. In addition, the sign of the asymmetry is the same in all bins in common where $V_\ell(+) - V_\ell(-)$ is significant (40 bins).

Distance estimation choice. We see that the main difference when using different distance estimates is in the overall distance scale, which extends much farther for $1/\pi$, dist2, and dist3 (Fig. 4, first panel) than for dist1. Additionally, for these alternative distance estimates, the magnitude of the asymmetry in velocity suspiciously increases as a function of distance for all longitudes, reaching extreme values. (plotted in dark colours in the left top panel of Fig. 4). For instance, with dist2 $V_\ell(+) - V_\ell(-)$ has a median of 6.3 km s^{-1} and 24% of the bins show differences larger than 10 km s^{-1}. These large asymmetries could be due to an overestimation of the distance, which leads to an overestimation of V_ℓ. This effect is only mildly observed for dist1 (but note the same effect at high Z in Fig. 2), hence, our preferred choice of this distance estimate. Despite these differences, our main results do not depend significantly on the distance estimate: the sign of the pattern is the same in 90%, 81%, and 91% of the significant bins when comparing dist1 with $1/\pi$, dist2, and dist3, respectively.

Parallax accuracy. As recommended in Arenou et al. (2017), a possible parallax bias of ~0.3 mas that could be non-uniform in the sky has to be considered in the analysis of TGAS data.

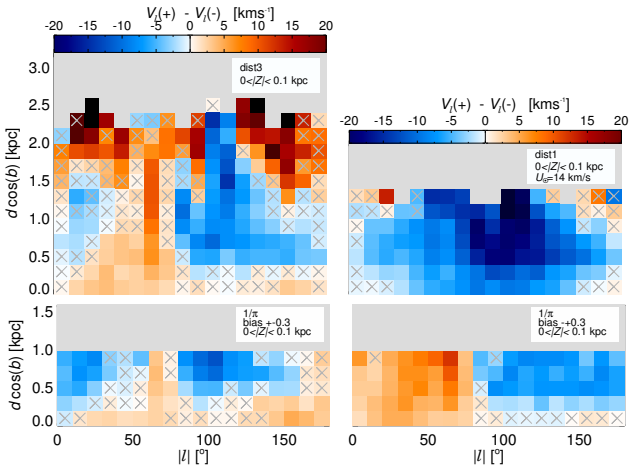

Fig. 4. Same as Fig. 1, but for dist3 (*left top panel*), assuming $U_\odot$ = 14 km s^{-1} (*right top panel*), correcting for an assumed systematic bias in the parallax of +0.3 mas for $\ell > 0$ and of −0.3 mas for $\ell < 0$ (*left bottom panel*), and the reverse bias (*right bottom panel*). The *bottom panels* are cut at 1 kpc where the error in distance starts to be larger than the bin size.

Here we see that the distances with this systematic error taken into account from Astraatmadja & Bailer-Jones (2016) slightly shorten the distance scale but do not change the asymmetry. We also repeated our calculations using $1/\pi$ and correcting for a systematic bias, that is, effectively adding 0.3 mas to or subtracting 0.3 mas from the parallax. We show here two cases where we added −0.3 mas for $\ell > 0$ and +0.3 mas for $\ell < 0$, and the reverse (Fig. 4, bottom panels). We note that these are the worst-case scenarios in which the bias contributes most to the velocity asymmetry in Eq. (2). In these cases the asymmetry pattern changes slightly, especially towards the inner and outer parts of the Galaxy, but is preserved overall. We conclude that the presumed bias in parallax cannot be responsible for the global velocity asymmetry that is observed. We also note that the negative sign of the asymmetry at $l \sim 100°$ does not change even under the more extreme systematics considered here. This is therefore a very robust result that models of the asymmetry must reproduce.

Correlation between parallax and proper motion. The astrometric correlations can be of up to ±1 in certain sky regions in the TGAS data (see Fig. C.1 in Arenou et al. 2017). However, the velocity asymmetry is not induced by these correlations. We have tested this by first adding uncorrelated noise equal to three times the standard errors reported in the catalogue, which is enough to break the correlations. We only observe little changes that might well be due to introducing larger errors and not to the correlations, but the overall asymmetry pattern is preserved. Secondly, we added extra correlated noise using the individual reported standard errors and setting all astrometric correlations i, j to $\rho_{ij} = \pm 1$ (keeping its original sign). This does not increase the observed velocity asymmetry.

Sky coverage, completeness, and extinction. The TGAS catalogue is incomplete and has a non-uniform sky coverage (e.g. see Fig. 5 of Arenou et al. 2017). Owing to this and to extinction, there are differences in the number of observed stars in the symmetric bins $(\ell, d\cos(b))$ and $(-\ell, d\cos(b))$. However, these will not bias the median transverse velocity, but only change its precision, assuming there are no additional selection effects. Moreover, if in the pairs of bins there were a difference in the vertical distribution of stars (for instance a different median Z at positive and negative longitudes), the measured asymmetry could be due to a different V_ℓ as a function of Z, which is expected in

an axisymmetric galaxy. However, the velocity changes with Z in the thin layer we selected (200 pc) are much smaller than the velocity asymmetry we measure: taking Eq. (13) of Bond et al. (2010), the velocity at $Z = 0$ would change only by $1\,\mathrm{km\,s^{-1}}$ at $Z = 100$ pc.

Assumption of $U_\odot$. Ideally, one should fit the non-axisymmetry model and the value of $U_\odot$ at the same time to the observed velocity asymmetry. Here our analysis requires an assumption for $U_\odot$ (Eq. (2)). However, we note that a different $U_\odot$ cannot completely smooth the asymmetry at all Galactic longitudes because the term $-2U_\odot \sin|\ell|$ always has the same sign. It will only modify the pattern and sign of the asymmetry. When we use $U_\odot = 14\,\mathrm{km\,s^{-1}}$ (Schönrich 2012), for instance, the asymmetry becomes negative everywhere (Fig. 4 top right panel), reaching values down to $-25\,\mathrm{km\,s^{-1}}$ and with 34% of the bins with asymmetries as large as $10\,\mathrm{km\,s^{-1}}$, but does not disappear. On the other hand, one can estimate a value of $U_\odot$ from the data by averaging the quantity $U_\odot = \frac{\widetilde{\kappa d\mu_{\ell*}}\,(\ell>0) - \widetilde{\kappa d\mu_{\ell*}}\,(\ell<0)}{2\sin|\ell|}$ for all bins (i.e. assuming that $V_\ell(+) - V_\ell(-) = 0$, in other words, that there is no net contribution from non-axisymmetries). This value is $U_\odot = 8.3 \pm 0.6\,\mathrm{km\,s^{-1}}$, and thus, for our choice of $U_\odot = 9\,\mathrm{km\,s^{-1}}$ the total net asymmetry is the smallest compared to other values.

To conclude, with the information currently available to us on the quality and limitations of the TGAS data and of our method, the measurement of the velocity asymmetry is robust.

6. Discussion and conclusions

We have detected velocity asymmetries when comparing the median transverse velocity in Galactic longitude for positive and negative longitudes using the *Gaia*-TGAS catalogue following a model-independent approach. The sign of the velocity differences follows a pattern that depends on the distance and direction. The velocity asymmetry reaches values higher than $10\,\mathrm{km\,s^{-1}}$ for 7% of the region we studied. This asymmetry, which extends to all distances and directions we probed, indicates that the stellar motion in the disk is highly non-axisymmetric.

Part of the asymmetry (in the direction of the outer disk) is present for all the stellar types considered here. This points towards a common dynamical origin of the asymmetry. The differences seen for the young sample (not yet phase-mixed) can be due to imprints of the velocities at birth or structures such as the Gould belt (Lesh 1968; Comeron & Torra 1994). The differences when comparing dwarfs with giant stars could be due to the same perturbation acting differently on different mean ages.

The values that we find for the asymmetry magnitude are similar to previous determinations of streaming motion. For example, star-forming regions deviate from rotation by typically $10\,\mathrm{km\,s^{-1}}$ (Reid et al. 2014; Honma et al. 2012; Rygl et al. 2012). In external galaxies, radial streaming motions of $7\,\mathrm{km\,s^{-1}}$ are observed (Rix & Zaritsky 1995). For the Milky Way, velocity gradients in the radial direction are $3\,\mathrm{km\,s^{-1}\,kpc^{-1}}$ (Siebert et al. 2011) and fluctuations with amplitude of $10\,\mathrm{km\,s^{-1}}$ have been measured (Bovy et al. 2015).

A16 studied the asymmetries in transverse velocity for a series of disk simulations with spiral structure. Some models followed the tight-winding-approximation (TWA) and some were N-body models. The magnitude of the typical velocity asymmetries of the models were of the order of $\sim 2\,\mathrm{km\,s^{-1}}$ but up to $10\,\mathrm{km\,s^{-1}}$, which means that they resemble those found here (see also Faure et al. 2014; Grand et al. 2016, for alternative but similar predictions). However, the asymmetry patterns changed with a distance scale larger than in the data, except for the model of transient arms. Furthermore, the particular pattern of the observed asymmetry, and in particular, its sign, does not follow what we saw in the vast majority of models that were built to resemble the spiral structure of the Galaxy (see Fig. 6 of A16, but note the different distance range). However, a quantitative fit of the model exploring the whole range of spiral parameters is necessary to draw clear conclusions (Antoja et al., in prep.).

This asymmetry could also be attributed to the Galactic bar that can cause the velocities to deviate from axisymmetry by about $5-10\,\mathrm{km\,s^{-1}}$ near the Sun (Monari et al. 2014; Bovy et al. 2015), which is compatible with the data here. A perturbation from a satellite could excite breathing or other disk modes (Gómez et al. 2013; Widrow et al. 2014), but little attention is given to its effects on the in-plane velocities. An elliptic potential induced by a non-spherical halo can also perturb the in-plane velocities (Kuijken & Tremaine 1994). How well these other models reproduce the observed asymmetry needs to be investigated. Several agents may contribute simultaneously to it, creating a quite intricate Galaxy disk. We hope to decipher it with the advent of new data (*Gaia* DR2 and follow-up surveys) and models that combine internal and external agents driving the evolution of the Milky Way disk.

Acknowledgements. We thank the referee for the careful reading and advice. This work was supported by the MINECO (Spanish Ministry of Economy) – FEDER through grant ESP2016-80079-C2-1-R and ESP2014-55996-C2-1-R and MDM-2014-0369 of ICCUB (Unidad de Excelencia "Maria de Maeztu"). This work has made use of data from the European Space Agency (ESA) mission *Gaia* (`https://www.cosmos.esa.int/gaia`), processed by the *Gaia* Data Processing and Analysis Consortium (DPAC, `https://www.cosmos.esa.int/web/gaia/dpac/consortium`). Funding for the DPAC has been provided by national institutions, in particular the institutions participating in the *Gaia* Multilateral Agreement. We also thank the *Gaia* Project Scientist Support Team, DPAC and Anthony Brown for the PyGaia code that has been used in this research.

References

Antoja, T., Roca-Fàbrega, S., de Bruijne, J., & Prusti, T. 2016, A&A, 589, A13
Arenou, F., Luri, X., Babusiaux, C., et al. 2017, A&A, 599, A50
Astraatmadja, T. L., & Bailer-Jones, C. A. L. 2016, ApJ, 833, 119
Bond, N. A., Ivezić, Ž., Sesar, B., et al. 2010, ApJ, 716, 1
Bovy, J. 2017, MNRAS, 468, L63
Bovy, J., Bird, J. C., García Pérez, A. E., et al. 2015, ApJ, 800, 83
Carlin, J. L., DeLaunay, J., Newberg, H. J., et al. 2013, ApJ, 777, L5
Chen, B., Stoughton, C., Smith, J. A., et al. 2001, ApJ, 553, 184
Coşkunoğlu, B., Ak, S., Bilir, S., et al. 2011, MNRAS, 412, 1237
Comeron, F., & Torra, J. 1994, A&A, 281, 35
Faure, C., Siebert, A., & Famaey, B. 2014, MNRAS, 440, 2564
Gaia Collaboration (Brown, A. G. A., et al.) 2016a, A&A, 595, A2
Gaia Collaboration (Prusti, T., et al.) 2016b, A&A, 595, A1
Gómez, F. A., Minchev, I., O'Shea, B. W., et al. 2013, MNRAS, 429, 159
Grand, R. J. J., Springel, V., Kawata, D., et al. 2016, MNRAS, 460, L94
Honma, M., Nagayama, T., Ando, K., et al. 2012, PASJ, 64, 136
Kuijken, K., & Tremaine, S. 1994, ApJ, 421, 178
Lesh, J. R. 1968, ApJS, 17, 371
Lindegren, L., Lammers, U., Bastian, U., et al. 2016, A&A, 595, A4
Michalik, D., Lindegren, L., & Hobbs, D. 2015, A&A, 574, A115
Monari, G., Helmi, A., Antoja, T., & Steinmetz, M. 2014, A&A, 569, A69
Pasetto, S., Grebel, E. K., Zwitter, T., et al. 2012, A&A, 547, A70
Pickles, A., & Depagne, É. 2010, PASP, 122, 1437
Reid, M. J., Menten, K. M., Brunthaler, A., et al. 2014, ApJ, 783, 130
Rix, H.-W., & Zaritsky, D. 1995, ApJ, 447, 82
Rygl, K. L. J., Brunthaler, A., Sanna, A., et al. 2012, A&A, 539, A79
Schönrich, R. 2012, MNRAS, 427, 274
Siebert, A., Famaey, B., Minchev, I., et al. 2011, MNRAS, 412, 2026
Widrow, L. M., Gardner, S., Yanny, B., Dodelson, S., & Chen, H.-Y. 2012, ApJ, 750, L41
Widrow, L. M., Barber, J., Chequers, M. H., & Cheng, E. 2014, MNRAS, 440, 1971